

Evaluation of Radiation Performance of Wearable Antennas for RF Energy Harvest

Xinhui Zhang*, Huapeng Zhao

University of Electronic Science and Technology of China, Chengdu, China

Abstract

In this work, the equivalent model of wearable antennas for radio frequency (RF) energy harvest is established by integral equation method, and the proposed equivalent model can be used to perform integrated simulation with human model for obtaining the installed radiation performance. Compared with the original model, equivalent model has a simpler structure and it can thus greatly reduce the computing time and memory cost of integrated simulation. It is useful and helpful for efficiently evaluating the radiation performance of wearable antennas in RF energy harvest system.

1 Introduction

The applications of low-power and miniaturized wearable electronic devices promote the development of wireless body area network (WBAN) technology, WBAN has a strong potential for healthcare, entertainment, identification systems, sport, smart home, and military applications [1, 2]. In order to ensure the implementation of the above applications, some high-performance and intelligent wearable electronic devices need to be installed on the human body [3], which requires a stable, reliable and real-time power supply to power these electronic devices. The most common way of power supply is to use batteries to power electronic devices, but batteries need to be recharged or replaced due to finite capacity of batteries, which is inconvenient and costly. Besides, with the rapid development of wireless power transfer (WPT) technology, harvesting energy from the ambient environment to perpetually power electronic devices is a promising solution [4], because there are a series of RF signals in ambient environment such as TV, radio, and WiFi signals, which can be harvested to power wearable electronic devices. Wearable antennas are attractive for WBAN because of its flexible geometry, and they can be used for RF energy harvest to power wearable electronic devices [5, 6].

The radiation performance of wearable antennas is an important factor affecting the efficiency of RF energy harvest. The human body is an inhomogeneous dispersion medium, which will change the radiation performance of wearable antennas installed on human body, so the installed radiation performance of wearable antennas needs to be evaluated. There are two methods to evaluate the installed radiation performance of wearable antennas. The first method is to actually test the radiation patterns of

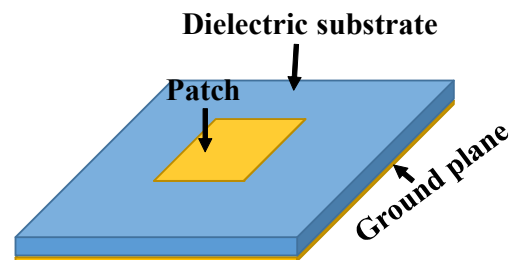


Figure 1. Illustration of a common patch antenna.

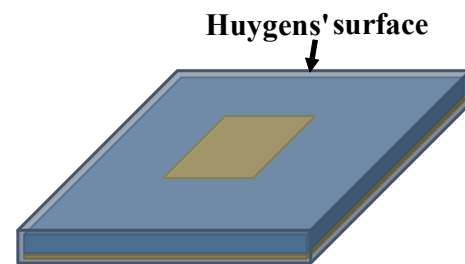


Figure 2. Huygens' surface encloses the patch antenna.

wearable antennas installed on the human body model, but actual test is very expensive and also has requirements on the test site. The second method is the integrated simulation of wearable antennas and human body model, which is hindered by long simulation time for complex material and multi-scale geometry [7]. Besides, the design details of wearable antennas may be unknown for RF energy harvest system engineers, which further hinders the integrated simulation.

For overcoming the limitations of integrated simulation, the equivalent modeling method is proposed, which is widely used in the near field prediction of the printed circuit board and evaluation of radiation performance of the vehicle antenna [8, 9]. In this work, the equivalent model of wearable antennas is established by integral equation method, because the integral equation method does not require that the distribution of radiation source be far away from the metal edges. Compared with the original model, the integrated simulation of equivalent model and human model needs less computing time and memory cost.

2 Establishment of Equivalent Model

Patch antennas are widely used in the manufacture of wearable antennas because of its low profile, low back lobe, and ease of realizing conformal with human body. Figure 1 shows the structure of a common patch antenna, which is made up of patch, dielectric substrate and ground plane. As shown in Figure 2, according to Huygens' principle [10], the patch antenna can be enclosed by a closed Huygens' surface. Equivalent electric and magnetic currents are placed on the Huygens' surface, and they can generate the same radiation field in the region outside Huygens' surface as the original model. Equivalent electric and magnetic current can be written as follows

$$\vec{J}(\vec{r}') = \hat{n}(\vec{r}') \times \vec{H}(\vec{r}') \quad (1)$$

$$\vec{M}(\vec{r}') = \vec{E}(\vec{r}') \times \hat{n}(\vec{r}') \quad (2)$$

where \vec{J} and \vec{M} represent equivalent electric and equivalent magnetic current, respectively, \vec{r}' is the source position vector, \hat{n} is the unit external normal vector of the Huygens' surface, and \vec{E} and \vec{H} are the electric field and magnetic field on the Huygens' surface, respectively.

It is not easy to directly measure the electric and magnetic field on the Huygens' surface, so two near field scanning planes far away from the patch antenna are selected to solve the equivalent source of the antenna, as shown in Figure 3. By the Green's function in free space, the electric field on scanning planes can be expressed as the following integral [10]:

$$\vec{E}(\vec{r}) = -jk\eta \iint_{S_H} \left[1 + \frac{1}{k^2} \nabla \nabla \cdot \right] \left[\vec{J}(\vec{r}') G(\vec{r}, \vec{r}') \right] dS' - \iint_{S_H} \nabla G(\vec{r}, \vec{r}') \times \vec{M}(\vec{r}') dS' \quad (3)$$

where \vec{r} is the position vector of field point, \vec{E} is the electric field on scanning planes, k is the wavenumber in free space, η is the intrinsic impedance in free space, S_H denotes the Huygens' surface, and $G(\vec{r}, \vec{r}')$ is Green's function in free space, which can be written as

$$\vec{G}(\vec{r}, \vec{r}') = \frac{e^{-jk|\vec{r}-\vec{r}'|}}{4\pi|\vec{r}-\vec{r}'|} \quad (4)$$

Equation (3) establishes the relationship between the equivalent source and the electric field on the scanning planes. By RWG basis function and point matching [10], the integral equation (3) can be transformed into the following matrix equation:

$$\mathbf{G}\mathbf{x} = \mathbf{f} \quad (5)$$

where \mathbf{f} is the vector filled with electric field on the scanning planes, \mathbf{x} is the vector consisting of the expansion coefficients of equivalent electric and magnetic current, and \mathbf{G} is the matrix representing the relationship between equivalent source and electric field. When the electric field data on the scanning planes are obtained, the equivalent source can be calculated by solving matrix equation (5).

3 Numerical Results

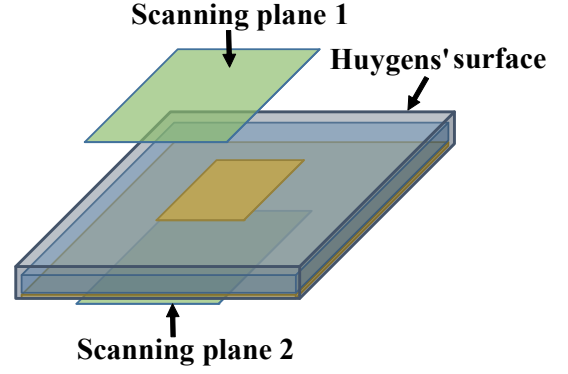


Figure 3. Two near field scanning planes are selected.

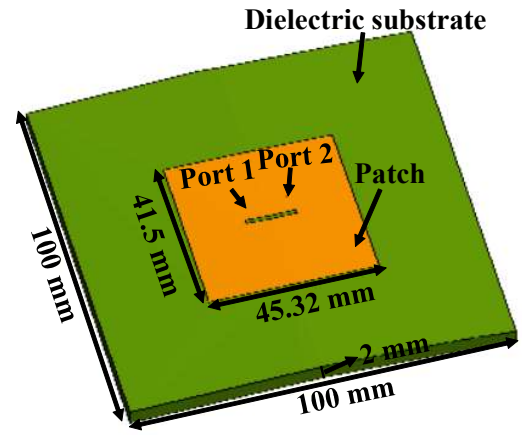


Figure 4. The geometric structure of a conformal wearable antenna.

The geometric structure of a conformal wearable antenna is shown in Figure 4, and more details about it can be found in [11]. The relative permittivity of dielectric substrate is 1.53, and its loss tangent is 0.0012. The working frequency of the wearable antenna is 2.45 GHz. Two electric field scanning planes shown in Figure 3 are selected. Scanning plane 1 with an area of 200 mm×200 mm is located at 20 mm above the wearable antenna, and scanning plane 2 with an area of 200 mm×200 mm is located at 20 mm below the wearable antenna. \mathbf{f} in (5) can be filled with the simulated electric field data. Finally, the equivalent model of wearable antenna can be solved by (5).

In order to verify the accuracy of equivalent model, a validation plane with an area of 400 mm×400 mm is selected, and it is located at 60 mm above the antenna. The electric field on the validation plane is calculated by the original model and equivalent model, respectively, and the relative error between the two methods are given in Table 1. It can be seen from Table 1 that the electric field on the validation plane calculated by the equivalent model is very consistent with that calculated by the original model, which indicates the good accuracy of equivalent model. In addition, the radiation patterns calculated by original model and equivalent model are shown in Figure 5, where

Table 1. The relative error of electric field on the validation plane calculated by two methods.

	Amplitude	Phase
E_x	0.76 %	0.65 %
E_y	0.13 %	0.13 %
E_z	0.26 %	0.12 %

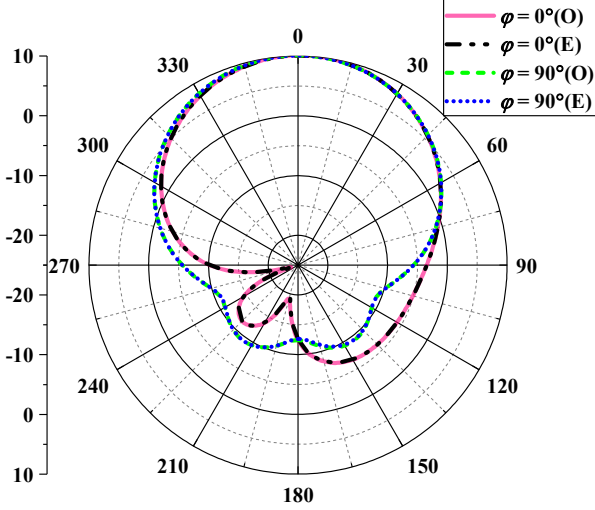


Figure 5. Radiation patterns of the wearable antenna calculated by the original model and the equivalent model.

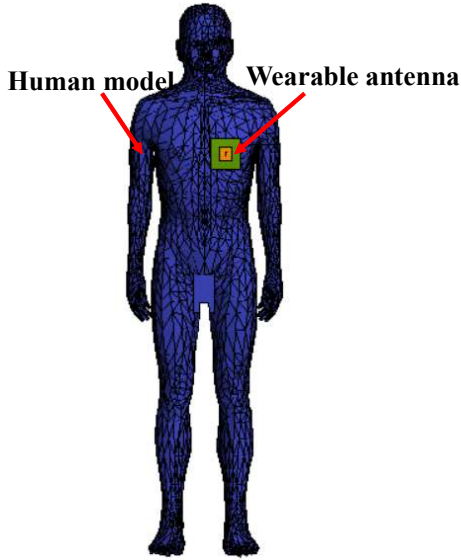


Figure 6. The wearable antenna is installed on the human body model.

“O” and “E” represent the original model and the equivalent model, respectively. According to Figure 5, the radiation patterns calculated by the equivalent model are consistent with that calculated by the original model.

In order to illustrate the effectiveness and accuracy of the integrated simulation of the equivalent model and the

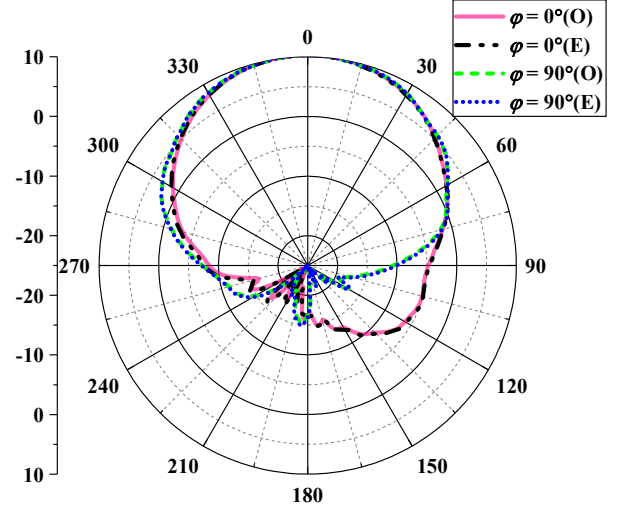


Figure 7. Radiation patterns of the wearable antenna installed on the human body model.

Table 2. Comparison of computing time and memory cost between original model and equivalent model.

	Computing Time	Memory Cost
Original model	7433.37 s	6.26 GB
Equivalent model	3595.79 s	5.46 GB

human body model, as shown in Figure 6, a human body model with the size of 260 mm×500 mm×1840 mm is built. Its relative permittivity is 40.43, conductivity is 1.59 S/m, and the density is 1125 kg/m³. The wearable antenna is installed on the chest of human body model, and the installed radiation patterns are calculated by using the original model and the equivalent model, respectively. The calculated results are shown in Figure 7, and it can be seen that the installed radiation patterns calculated by equivalent model are in good agreement with that calculated by the original model. Table 2 also compares the computing time and memory cost of the original model and equivalent model. It can be seen that, compared with the original model, the equivalent model saves 51 % of computing time and 0.8 GB of memory cost. Therefore, the equivalent model can improve the efficiency of integrated simulation. This is because there are no small-scale structures in the equivalent model, which will not cause multi-scale problems.

4 Conclusion

In this work, an equivalent model of wearable antenna has been established by integral equation method, and it can be used to perform the integrated simulation with human body model for obtaining the installed radiation patterns. Compared with the original model, the equivalent model can save 51 % of computing time and 0.8 GB of memory cost due to its simpler structure. It is very useful for fast radiation performance evaluation of wearable antennas in RF energy harvest system.

5 Acknowledgements

This work was supported by Sichuan Science and Technology Program under grant No. 2021YFH0070.

6 References

1. V. Talla, S. Pellerano, H. Xu, A. Ravi and Y. Palaskas, "Wi-Fi RF energy harvesting for battery-free wearable radio platforms", *2015 IEEE International Conference on RFID*, San Diego, CA, 2015.
2. N. Chahat, M. Zhadobov, L. Le Coq and R. Sauleau, "Wearable Endfire Textile Antenna for On-Body Communications at 60 GHz," *IEEE Antennas and Wireless Propagation Letters*, **11**, 2012, pp. 799-802, doi:10.1109/LAWP.2012.2207698.
3. D. He, S. Zeadally, N. Kumar and J. Lee, "Anonymous Authentication for Wireless Body Area Networks with Provable Security," *IEEE Systems Journal*, **11**, 4, December 2017, pp. 2590-2601, doi:10.1109/JSYST.2016.2544805.
4. D. Ma, G. Lan, M. Hassan, W. Hu and S. K. Das, "Sensing, Computing, and Communications for Energy Harvesting IoTs: A Survey," *IEEE Communications Surveys & Tutorials*, **22**, 2, 2020, pp. 1222-1250, doi:10.1109/COMST.2019.2962526.
5. K. W. Lui, O. H. Murphy and C. Toumazou, "A Wearable Wideband Circularly Polarized Textile Antenna for Effective Power Transmission on a Wirelessly-Powered Sensor Platform," *IEEE Transactions on Antennas and Propagation*, **61**, 7, July 2013, pp. 3873-3876, doi:10.1109/TAP.2013.2255094.
6. S. Adami et al., "A Flexible 2.45-GHz Power Harvesting Wristband with Net System Output From -24.3 dBm of RF Power," *IEEE Transactions on Microwave Theory and Techniques*, **66**, 1, Jan 2018, pp. 380-395, doi:10.1109/TMTT.2017.2700299.
7. M. Li and W. C. Chew, "Multiscale Simulation of Complex Structures Using Equivalence Principle Algorithm with High-Order Field Point Sampling Scheme," *IEEE Transactions on Antennas and Propagation*, **56**, 8, August 2008, pp. 2389-2397, doi:10.1109/TAP.2008.926785.
8. H. Zhao, S. Tao, Z. Chen and J. Hu, "Sparse Source Model for Prediction of Radiations by Transmission Lines on a Ground Plane Using a Small Number of Near-Field Samples," *IEEE Antennas and Wireless Propagation Letters*, **18**, 1, January 2019, pp. 103-107, doi:10.1109/LAWP.2018.2882132.
9. H. Zhao, C. Li, Z. Chen and J. Hu, "Fast Simulation of Vehicular Antennas for V2X Communication Using the Sparse Equivalent Source Model," *IEEE Internet of Things Journal*, **6**, 4, August 2019, pp. 7038-7047, doi:10.1109/IIOT.2019.2913659.
10. W. C. Gibson, *The Method of Moments in Electromagnetics*. New York, NY, USA: Chapman & Hall, 2008.
11. L. Vallozzi, H. Rogier and C. Hertleer, "Dual Polarized Textile Patch Antenna for Integration into Protective Garments," *IEEE Antennas and Wireless Propagation Letters*, **7**, 2008, pp. 440-443, doi:10.1109/LAWP.2008.2000546.